J. Appl. Comput. Mech., 8(4) (2022) 1154-1162
DOI: 10.22055/JACM.2021.16703

ISSN: 2383-4536
jacm.scu.ac.ir

Shahid Chamran University of Ahvaz

Journal of Applied and Computational Mechanics

Research Paper

Free Convection of Micropolar Fluid over an Infinite Inclined Moving Porous Plate

A.K. Dash, S.R. Mishra

Department of Mathematics, Siksha O Anusandhan Deemed to be University, Khandagiri Square, Bhubaneswar, 751030, Odisha, India
Emails: ashisdash8247@gmail.com, satyaranjan_mshr@yahoo.co.in

Received March 02 2020; Revised April 22 2020; Accepted for publication May 02 2020.
Corresponding author: S.R. Mishra (satyaranjan_mshr@yahoo.co.in)

Abstract. The present paper analyzes free convective heat and mass transfer of non-conducting micropolar fluid flow over an infinitely inclined moving porous plate in the presence of heat source and chemical reaction. Moreover, the effect of thermal radiation is also taken care of in the same study. The present investigation is relevant to the fabrication system in industries corresponding to the materials composed with high-temperature. Similarity technique is adopted with similarity variable to transform the non-dimensional form of the partial differential equations into ordinary differential equations. To get the approximate solution of these transformed complex nonlinear set of ODEs we have employed fourth order Runge–Kutta method in conjunction with shooting technique. The validation of the present result as well as critical issues is addressed in the discussion section refereeing to the previously published work as a particular case. The behavior of physical parameters governs the flow phenomena are displayed via graphs and tables.

Keywords: Micropolar fluid; Free convection; inclined plate; Heat source/sink; Chemical reaction; Runge-Kutta method.

1. Introduction

In the past, flow through porous media play a vital role in several industrial processes to get the final product as well as due to its practical applications such as nuclear waste disposal, thermal insulation etc., researchers have keen interest on the topic for the flow phenomena of various liquids. More extensively, natural convection encountered as an important application in several engineering problems like geothermal system, nuclear waste materials, etc. Similarly, mass transfer phenomena in various geometries embedding with porous material have large scale application in Engineering and Geophysics. Now, in present scenario, study on the magnetohydrodynamics has a major role in both the geophysical and astrophysical problem. To get a control over the various purposes such as thermal protection, pollution, breaking etc. the concept of electrically conducting MHD fluid vital in recent era. Many researchers studied the effect of magnetic field on the convection flow due to its large area of application. Free convection effect on the flow of MHD fluid is significant in aeronautical and chemical engineering processes etc. Many people have been working in these areas to understand fluid flow behavior.

Micropolar fluids are the particular form of non-Newtonian fluids with microstructure consisting of micro-costituents that undergoes rotation. These complex fluids with nonsymmetrical stress tensor, known as microorphic fluids. These fluids are very much important for Engineers and Scientists working in the field of hydrodynamics fluid problems. Physically they are made up of fluid particles where deformation of the particle is ignored are of randomly oriented or spherical particles suspended in viscous medium. The theory of micropolar fluids was initially described by Eringen [1]. He has suggested that micropolar fluid properties are influenced by local motion of the material particles which possess local inertia. He has extended his simple theory of micropolar fluid to thermomicrofluids by including heat conduction and heat dissipation effect [2]. Ahmadi [3] examined the flow of a polar fluid past a vertical plate. Carragher et al. [4] have studied heat transfer in continuous stretching sheet. Chim et al. [5] examined a mixed convective flow of time-independent vertical impermeable surface equipped with porous material in which linear variation in temperature profile is considered. Chamkha[6] studied the flow of an electrically conducting fluid through a vertical plate in presence of porous medium and magnetic field. Beg et al. [7] and Rawat et.al [8] investigated the steady flow comprising of dissipative heat energy in polar fluid for the flow phenomena in a Darcy regime. Hayat et al. [9] have studied the flow of mixed convection boundary layer for heat and mass transfer characteristics in a flow of visco-elastic fluid, with the influence of Dufour and Soret effects. Mukhopadhyay [10] investigated the mechanism of heat radiation and transfer on time-dependent flow through a stretching surface via porous medium. Rahman et al. [11] studied MHD convective flow in conjunction with heat generation/absorption of a polar fluid in a continuously moving plate. Reddy et al. [12] have studied the effects of thermo-diffusion on a time-dependent conducting free convective flow past an infinite vertical porous plate. Rawat et al. [13] have studied the flow phenomena of micropolar fluid in Darcy Forchheimer porous medium through a linearly stretching sheet. Tripathy et al. [14] investigated the behavior of chemical reaction on the natural convection of MHD micropolar fluid in a vertical

Published online: March 23 2021

surface. They have employed numerical technique for the solution of complex governing equations. They have also considered the behavior of heat radiation along with the dissipative heat energy incorporating in energy transfer equation. Further, Tripathy et al. [15] and Mishra et al. [16] have proposed their study with the various effects like non-uniform heat source and Soret on the hydromagnetic flow of micropolar fluid. In their studies, as a consequence a thermal gradient, a component flux appears which causes the effect of thermal diffusion known as Soret. The stagnation-point flow of micropolar fluid in a vertical surface for the effects of hear source for both the assisting and opposing cases is presented by Baag et al. [17]. Numerical treatment is deployed in their study to tackle the coupled nonlinear equations. Recently, Mishra et al. [18] presented their worn for the influence of thermal radiation on the hydromagnetic flow of micropolar fluid.

To the best of our knowledge, and from above short discussion of earlier studies it is necessary to study the effect chemical reaction of the flow that is free from convection and transfer phenomena of micropolar fluid over an inclined porous plate in conjunction with heat source/sink. Therefore, keeping this in mind, the work of Ram Reddy et al. [19] is extended by incorporating some additional terms such as heat source/sink in the heat transfer equation and chemical reaction in the mass transfer equation respectively. For the solution of current problem we use numerical method. Those results for various values of physical parameters governing the flow phenomena are obtained and presented through graphs and tables.

2. Mathematical modeling and formulation

2.1. Formulation of the problem

Consider a steady, two-dimensional flow of polar fluid over an infinite inclined $(0^\circ \le \alpha \le 90^\circ)$ plate embedding with porous is moving continuously. In addition to that, the influences of uniform heat source/sink and chemical reaction are considered in the present investigation. In Fig. 1 the flow details with coordinate system is illustrated. The angles $0^\circ, 90^\circ$ and inclination in between that show respectively the vertical, horizontal and plate with some inclination. The flow is taken place along the sheet i.e. x-direction, and y-axis normal to it. T_∞ and C_∞ are free stream temperature and concentration respectively. Here, $T_f > T_\infty$ stands for assisting and $T_f < T_\infty$ for opposing flow and v_w represents the suction/injection velocity. In order to keep the boundary condition simple, the hole size assumed to be much larger than the microscopic length.

By the above assumptions, governing boundary layer equations (see Ram Reddy et al. [19]) for steady convective flow are:

$$\frac{\partial u'}{\partial x'} + \frac{\partial v'}{\partial y'} = 0 \tag{1}$$

$$u\frac{\partial u'}{\partial x'} + v'\frac{\partial u'}{\partial y'} = \left(\frac{\mu + k}{\rho}\right)\frac{\partial^2 u'}{\partial y'^2} + g\beta_T(T - T_\infty)\cos\alpha + g\beta_c(C - C_\infty)\cos\alpha + \frac{k}{\rho}\frac{\partial N'}{\partial y'} \tag{2}$$

$$u'\frac{\partial N'}{\partial x'} + v'\frac{\partial N'}{\partial y'} = \frac{\gamma}{\rho j'}\frac{\partial^2 N'}{\partial y'^2} - \frac{k}{\rho j'}\left(\frac{\partial u'}{\partial y'} + 2N'\right) \tag{3}$$

$$u'\frac{\partial T}{\partial x'} + v'\frac{\partial T}{\partial y'} = \frac{\kappa}{\rho C_p}\frac{\partial^2 T}{\partial y'^2} - \frac{1}{\rho C_p}\frac{\partial q_r}{\partial y'} + \frac{Q}{\rho C_p}(T - T_\infty) \tag{4}$$

$$u'\frac{\partial C}{\partial x'} + v'\frac{\partial C}{\partial y'} = D\frac{\partial^2 C}{\partial y'^2} - K_r'(x')(C' - C_\infty) \tag{5}$$

The boundary conditions for the model are obtained from Reddy et al. [19]:

$$\begin{aligned} &\text{at } y' = 0,\ u' = 0,\ v = v_w,\ N' = -n\frac{\partial u'}{\partial y'},\ \frac{\partial T}{\partial y'} = -\frac{h_f}{k}\left(T_f - T\right),\ C = C_w \\ &\text{as } y' \to \infty, u' \to 0, N' \to 0,\ T \to T_\infty,\ C \to C_\infty \end{aligned} \tag{6}$$

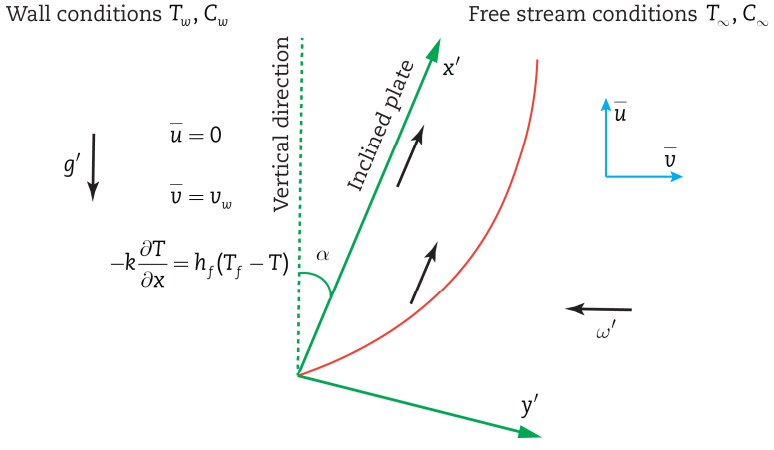

Fig. 1. Flow Geometry of the problem

Here u', x' -component and v', y' -component of velocity respectively. The microrotation component N' describes its relationship with the surface stress whose rotation is in the x' and y' axis. μ, the dynamic viscosity, ρ, the density, k, the vortex viscosity, β_T and β_c are coefficient of thermal expansion and concentration expansion, g', the acceleration, γ, material property, j' is the micro inertia per unit mass, T_∞ is the temperature of fluid close to the plate (wall) and T_∞ is the temperature far away from it, κ, thermal conductivity, p, the pressure, C_p, the specific heat, q_r, the heat flux, D, the mass diffusivity.

Introducing the following no-dimensional variables

$$\left.\begin{aligned} &x=\frac{x'}{L},\quad y=\frac{y'}{L}Gr^{1/4},\quad u=\frac{L}{\nu\sqrt{Gr}}u',\quad v=\frac{L}{\nu\, Gr^{1/4}}v',\ N=\frac{L^2}{\nu\, Gr^{3/4}}N' \\ &\theta=\frac{T-T_\infty}{T_f-T_\infty},\ \phi=\frac{C-C_\infty}{C_w-C_\infty}, Gr=\frac{g'\beta_T(T_f-T_\infty)L^3}{\nu^2} \end{aligned}\right\} \tag{7}$$

The radiative heat flux following Rosseland diffusion approximation, given by:

$$q_r=\frac{-4\bar{\sigma}}{3\bar{k}}\frac{\partial T'^4}{\partial y'} \tag{8}$$

Here $\bar{\sigma}$, Stefan-Boltzmann constant and $\bar{k}$, mean absorption coefficient. The linear form of the higher order of T'^4 can be expressed as:

$$T'^4\cong 4T_\infty'^3T-3T_\infty'^4 \tag{9}$$

Therefore equation (3), becomes

$$u'\frac{\partial T}{\partial x'}+v'\frac{\partial T}{\partial y'}=\frac{\kappa}{\rho C_p}\left(1+\frac{16\bar{\sigma}}{3\bar{k}\,\kappa}T_\infty^3\right)\frac{\partial^2 T}{\partial y'^2} \tag{10}$$

and hence introducing $u=\partial\psi/\partial y$, $v=-\partial\psi/\partial x$, ψ, the stream function into equations (2)- (5),

$$\frac{\partial\psi}{\partial y}\frac{\partial^2\psi}{\partial x\,\partial y}-\frac{\partial\psi}{\partial x}\frac{\partial^2\psi}{\partial y^2}=\left(\frac{1}{1-K}\right)\frac{\partial^3\psi}{\partial y^3}-\left(\frac{K}{1-K}\right)\frac{\partial N}{\partial y}+\frac{g'\beta_T(T_f-T_\infty)L^3}{\nu^2 Gr}\theta\cos\alpha+\frac{g'\beta_c(C_w-C_\infty)L^3}{\nu^2 Gr}\phi\cos\alpha \tag{11}$$

$$\frac{\partial\psi}{\partial y}\frac{\partial N}{\partial x}-\frac{\partial\psi}{\partial x}\frac{\partial N}{\partial y}=\left(\frac{2-K}{2-2K}\right)\frac{\partial^2 N}{\partial y^2}-\left(\frac{K}{1-K}\right)\left(2N+\frac{\partial^2\psi}{\partial y^2}\right) \tag{12}$$

$$\frac{\partial\psi}{\partial y}\frac{\partial\theta}{\partial x}-\frac{\partial\psi}{\partial x}\frac{\partial\theta}{\partial y}=\frac{1}{\mathrm{Pr}}(1+R)\frac{\partial^2\theta}{\partial y^2}+S\theta \tag{13}$$

$$\frac{\partial\psi}{\partial y}\frac{\partial\phi}{\partial x}-\frac{\partial\psi}{\partial x}\frac{\partial\phi}{\partial y}=\frac{1}{Sc}\frac{\partial^2\phi}{\partial y^2}-Kr\phi \tag{14}$$

where ν is the kinematic viscosity, $N=k/(\mu+k)$, the coupling number $(0\le N<1)$, $\mathrm{Pr}=\mu C_p/\kappa$ the Prandtl number, $Sc=\nu/D$ is the Schmidt number, $j=L^2/\sqrt{Gr}$, density of micro inertia and $R=16\bar{\sigma}T_\infty^3/3\bar{k}\kappa$, the radiation parameter.

Subjected to boundary conditions

$$\left.\begin{aligned} &\text{at}\ \ y=0\quad \left\{\frac{\partial\psi}{\partial y}=0,\frac{\partial\psi}{\partial x}=f_w, N=-n\frac{\partial^2\psi}{\partial y^2},\quad \frac{\partial\theta}{\partial y}=-\mathrm{Bi}(1-\theta),\ \phi=1\right. \\ &\text{as}\ \ y\to\infty\quad \left\{\frac{\partial\psi}{\partial y}\to 0,, N\to 0,\quad \theta\to 0,\ \phi\to 0\right. \end{aligned}\right\} \tag{15}$$

2.2. Analysis of Lie group transformation

The set of PDEs (11) - (14) subjected to the boundary conditions (12) is highly unmanageable and computationally expensive and therefore, the transformation into ODEs is obtained by the help of Lie group, a special case and whose numerical solution is better easier. As a result the number of independent variables is reduced. Following Uddin et al. [19] it is assumed that,

$$\Gamma:\begin{cases} x=e^{-\varepsilon c_1}x^*,\ y=e^{-\varepsilon c_2}y^*,\quad \psi=e^{-\varepsilon c_3}\psi^*,\quad N=e^{-\varepsilon c_4}N^*,\ \theta=e^{-\varepsilon c_5}\theta^*, \\ \phi=e^{-\varepsilon c_6}\phi^*, \beta_T=e^{-\varepsilon c_7}\beta_T^*,\ \beta_c=e^{-\varepsilon c_8}\beta_c^*,\ j=e^{-\varepsilon c_9}j^*,\ \gamma=e^{-\varepsilon c_{10}}\gamma^* \end{cases} \tag{16}$$

Here $\varepsilon\neq 0$, and all the $c_i's\,(i=1,2,.....10)$ are not zeros. We seek the values of $c_i's\,(i=1,2,.....10)$ such that equations (11) – (14) is invariant under these transformations as in [19]. They are connected as follows

$$\left.\begin{aligned} &c_1=c_3=c_4=c_7=c_8=c_9=c_{10} \\ &\text{and} \\ &c_2=c_5=c_6=0 \end{aligned}\right\} \tag{17}$$

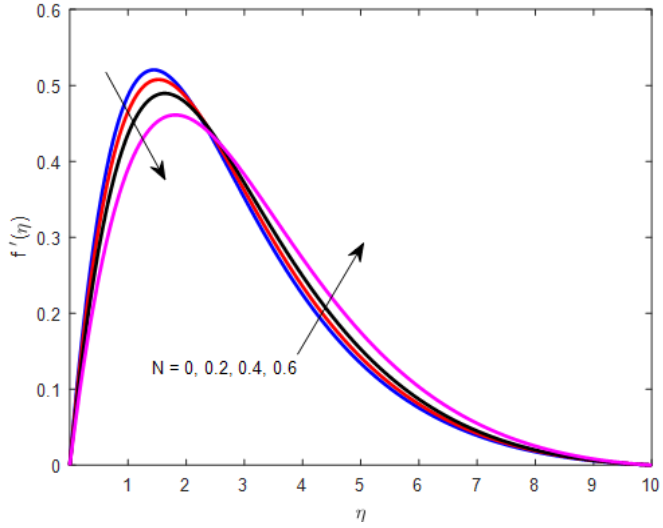

Fig. 2. Influence of N for $n=0.5, B=1, R=0.5, f_w=0.1, Sc=0.22,\ Kr=0,$ $Bi=0.1, Pr=0.71, S=0, \alpha=\pi/4$

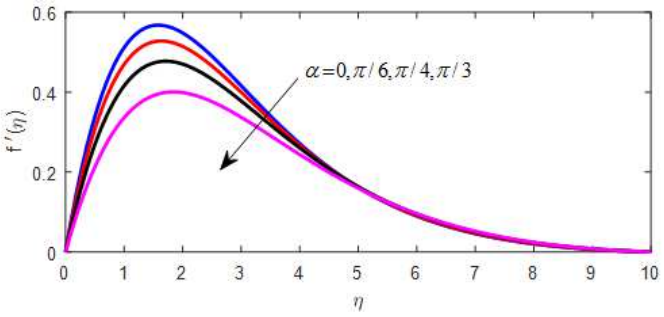

Fig. 3. Variation of α for $n=0.5, B=1, R=0.5,$ $f_w=0.1, Sc=0.22,\ Kr=0,\ Bi=0.1, Pr=0.71, S=0, N=0.5$

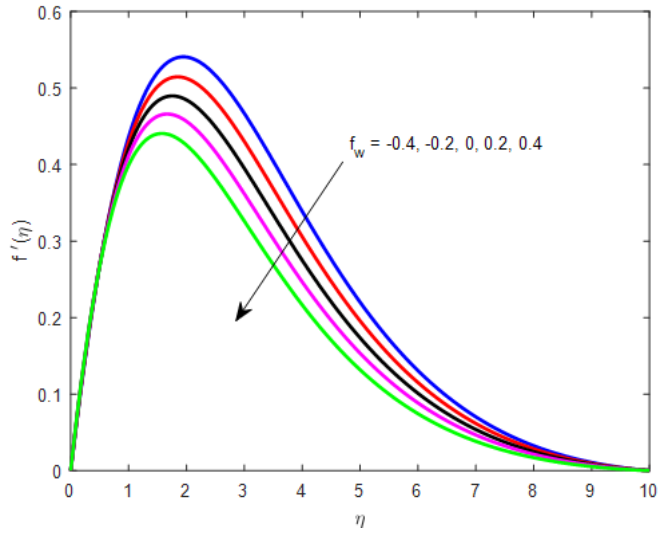

Fig. 4. Influence of f_w for $n=0.5, B=1, R=0.5,$ $\alpha=\pi/4, Sc=0.22,\ Kr=0,\ Bi=0.1, Pr=0.71, S=0, N=0.5$

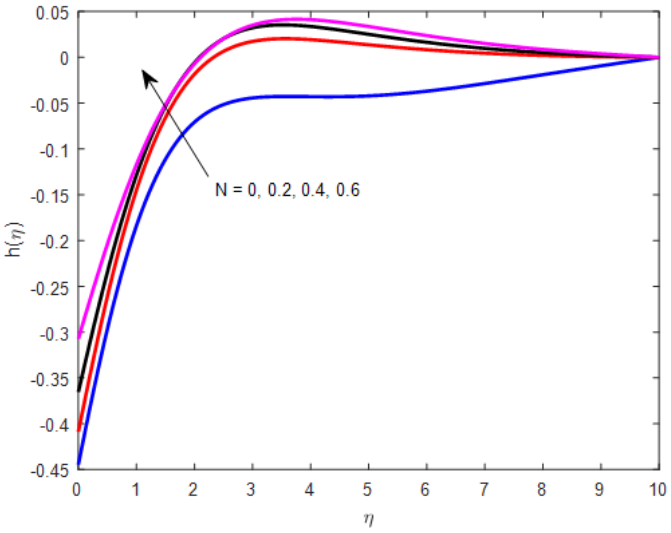

Fig. 5. Variation of N for $n=0.5, B=1, R=0.5,$ $f_w=0.1, Sc=0.22,\ Kr=0,\ Bi=0.1, Pr=0.71, S=0, \alpha=\pi/4$

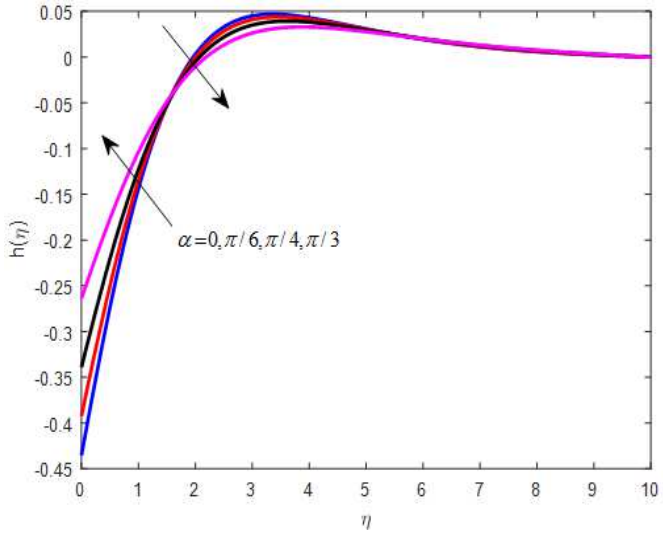

Fig. 6. Variation of α for $n=0.5, B=1, R=0.5,$ $f_w=0.1, Sc=0.22,\ Kr=0,\ Bi=0.1, Pr=0.71, S=0, N=0.5$

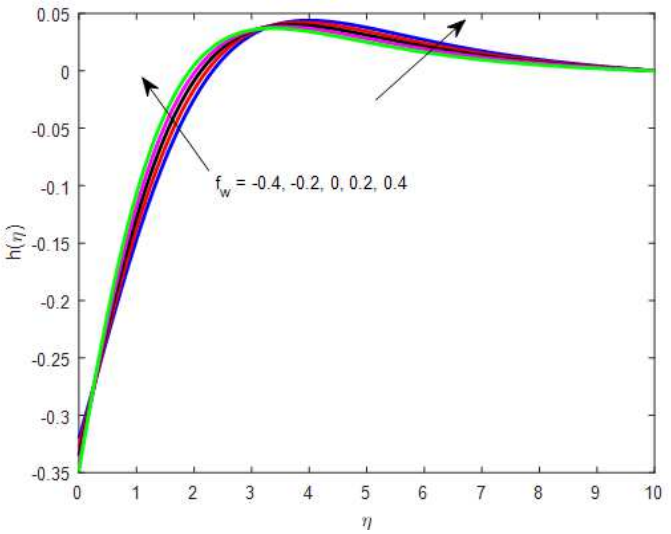

Fig. 7. Influence of f_w for $n=0.5, B=1, R=0.5, \alpha=\pi/4, Sc=0.22,$ $Kr=0,\ Bi=0.1, Pr=0.71, S=0, N=0.5$

The Characteristic equations are

$$\frac{dx}{c_1 x}=\frac{dy}{0}=\frac{dx}{c_1 x}=\frac{d\psi}{c_1\psi}=\frac{dN}{c_1 N}=\frac{d\theta}{0}=\frac{d\phi}{0}=\frac{d\beta_T}{c_1\beta_T}=\frac{d\beta_c}{c_1\beta_c}=\frac{d\,j}{c_1\,j}=\frac{d\,\gamma}{c_1\,\gamma} \tag{18}$$

Solving equation (18) we get

$$\left.\begin{aligned}&\eta=\mathrm{y},\quad \psi=\mathrm{x}\,f(\eta),\mathrm{N}=\mathrm{x}\,h(\eta),\ \beta_T=\beta_{T_0}\,\mathrm{x},\ \beta_c=\beta_{c_0}\,\mathrm{x},\\&\theta=\theta(\eta),\phi=\phi(\eta),\ j=j_0\,\mathrm{x},\ \gamma=\gamma_0\,\mathrm{x}\end{aligned}\right\} \tag{19}$$

where, β_{T_0},β_{c_0} are the volumetric coefficients, j_0,γ_0 are density of microinertia and the spin gradient viscosity.

Employing equation (19) into equations (11)-(14), the transformed equations with their boundary conditions are

$$\left(\frac{1}{1-N}\right)f'''+f\,f''-(f')^2+\left(\frac{N}{1-N}\right)h'+\theta\cos\alpha+\mathrm{B}\phi\cos\alpha=0 \tag{20}$$

$$\left(\frac{2-N}{2-2N}\right)\,h''+f\,h'-f'\,h-\left(\frac{N}{1-N}\right)(2h+f'')=0 \tag{21}$$

$$(1+\mathrm{R})\,\theta''+\mathrm{Pr}\,f\,\theta'+\mathrm{Pr}\,\mathrm{S}\theta=0 \tag{22}$$

$$\phi''+Sc\,f\,\phi'-Sc\,Kr\,\phi=0 \tag{23}$$

The boundary conditions (15) becomes

$$\left.\begin{aligned}&\text{at}\ \ \eta=0\quad\{\quad f(0)=f_w,f'(0)=0,h(0)=-n\,f''(0),\quad \theta'(0)=-Bi(1-\theta(0)),\ \phi(0)=1\\&\text{as}\ \ \eta\to\infty\ \{\quad f'(\infty)\to 0,,h(\infty)\to 0,\quad \theta(\infty)\to 0,\ \phi(\infty)\to 0\end{aligned}\right\} \tag{24}$$

where, $B=\beta_{c_0}(C_w-C_\infty)/\beta_{T_0}(T_f-T_\infty)$ is the buoyancy ratio parameter, $Bi=h_f\,L/kGr^{1/4}$, the Biot number, $f_w=-(L/\nu\,Gr^{1/4})v_w$, the suction/injection parameter, for suction $f_w>0$, injection $f_w<0$ and $f_w=0$ denotes surface is impermeable.

2.3. Coefficient of engineering interest

Here $\tau_w=(\mu+k)\partial\bar{u}/\partial\bar{y}+k\bar{N}|_{\bar{y}=0}$, the wall shear stress, $m_w=\gamma(\partial\bar{N}/\partial\bar{y})_{\bar{y}=0}$, wall couple stress, $q_w=-\kappa(\partial T/\partial\bar{y})_{\bar{y}=0}$, heat transfer coefficient and $q_m=-D(\partial C/\partial\bar{y})_{\bar{y}=0}$ is mass transfer coefficient in dimensional form. The non-dimensional skin friction $C_f=2\tau_w/\rho\bar{u}_*^2$, i.e. $C_f=2/\sqrt{Gr_{x'}}[(1-nN)/(1-N)]\,f''(0)$, non-dimensional wall couple stress coefficient $C_w=c_w/\rho\bar{u}_*^2$ i.e. $C_w=1/\sqrt{Gr_{x'}}[(2-N)/(2-2N)]\,h'(0)$, non-dimensional local Nusselt number $Nu=q_w/k(T_f-T_\infty)$ i.e. $Nu=-Gr_{x'}^{1/4}\,\theta'(0)$ and the non-dimensional local Sherwood number $Sh=q_m/D(C_w-C_\infty)$, i.e. $Sh=-Gr_{x'}^{1/4}\,\phi'(0)$, where $\bar{u}_*^2$ is the characteristic velocity and $Gr_{x'}=g'\beta_{T_0}(T_f-T_\infty)\,x'^3/\nu^2$ is the local Grashof number.

3. Results and discussion

Free convective flow of micropolar fluid past over an infinite inclined moving porous plate has been considered in the present investigation. The effects of thermal radiation, heat source/sink and chemical reactant species are also exhibited. The solution of set of ODEs is obtained numerically and the effects of various physical quantities are presented in graphs and their significance is also presented as follows. The computation for the contributing parameters on the flow phenomena are obtained and displayed via graphs (Figs.2-15) and tabular form (Table-1). However, several particular cases for validation of the present result in comparison to the work of Ram Reddy et al. [19] is presented in this section.

3.1. Velocity Profiles

Fig. 2 illustrates the effect of material parameter, N on the velocity profiles for fixed values of the parameters involved in the flow phenomena particularly in the absence of heat source/sink $(S=0)$ and chemical reaction parameter $(Kr=0)$. Both the case of Newtonian $(N=0)$ and non-Newtonian $(N>0)$ are presented in the figure. Here, N represents the coupling of both the linear and microrotational motion i.e. $N=k/(\mu+k)$. $N=0$ means the absence of micropolarity and it corresponds to the nonpolarity of the fluid. It is also seen that for Newtonian case, $N=0$, the velocity attains its maximum value near the plate within a region $\eta<2$ and the result is in good agreement with the results of Ram Reddy et al. [19]. Further, reverse effect is encountered for $\eta>2$, as fluid moves far from the plate to meet the desired boundary condition. Further, it is observed that the velocity profile decreases with increase in material parameter since the velocity moves farther away from the wall location. The influence of α, the inclination of the plate on the velocity profiles is well exhibited in Fig. 3 for the absence of both heat source/sink and chemical reaction parameter. On careful observation, it is remarked that velocity profile retards as the inclination of the plate increases. It is due to the fact that the increase in α, the gravity towards the flow field is more which opposes the velocity profile as a result profile retards. Fig. 4 portrays the behavior of suction on the velocity distribution in the absence of heat source/sink and fixed values of other pertinent parameters. It is seen that the deviation in the profile from the no suction region is approximately equal in magnitude for the case of suction/injection. The velocity profile decreases as an increase in strong suction $(f_w>0)$ and the trend becomes reversed for injection i.e. injection is favorable to enhance the profile significantly. But near the plate $\eta<1$ there is no significant increase/decrease is remarked. The reason is straight forward i.e. in the impermeable surface the surface velocity becomes zero and with an increase in an external velocity near the wall due to permeable surface retards the fluids velocity as well.

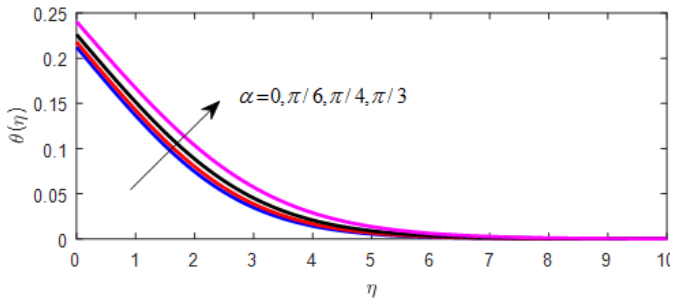

Fig. 8. Variation of α for $n=0.5, B=1, R=0.5,$ $f_w=0.1, Sc=0.22,\ Kr=0,\ Bi=0.1, Pr=0.71, S=0, N=0.5$

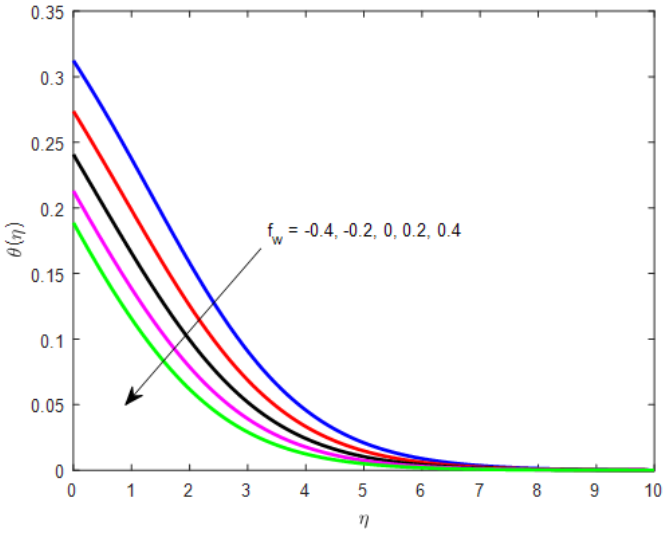

Fig. 9. Influence of f_w for $n=0.5, B=1, R=0.5,$ $\alpha=\pi/4, Sc=0.22,\ Kr=0,\ Bi=0.1, Pr=0.71, S=0, N=0.5$

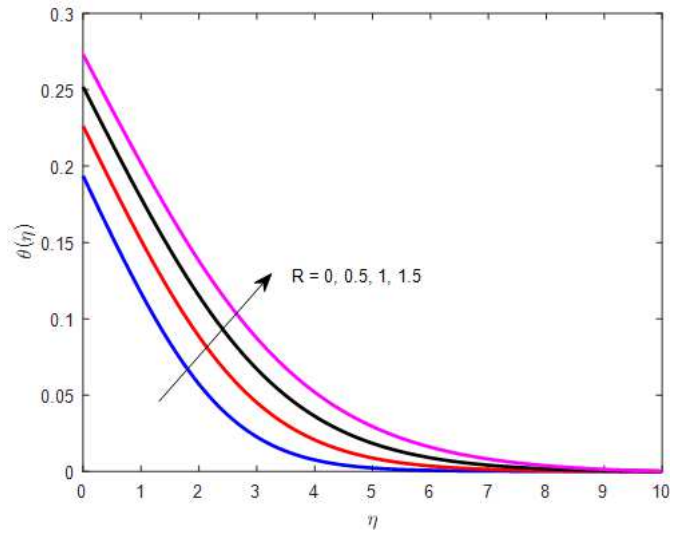

Fig. 10. Effect of R for $n=0.5, B=1, f_w=0.1,$ $\alpha=\pi/4, Sc=0.22,\ Kr=0,\ Bi=0.1, Pr=0.71, S=0, N=0.5$

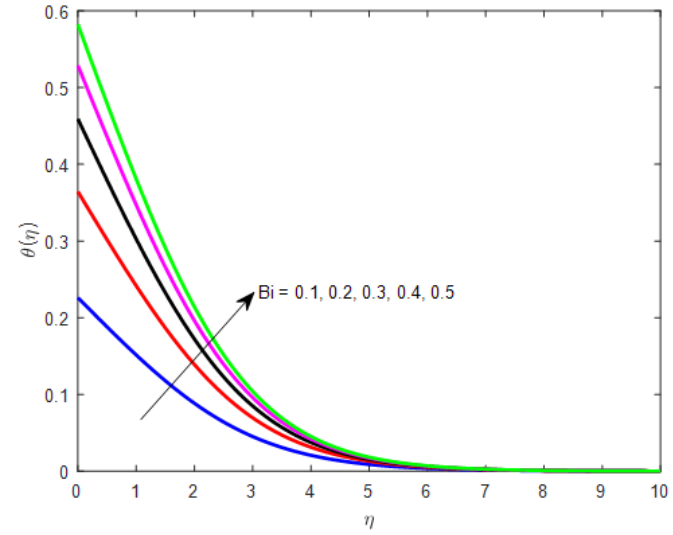

Fig. 11. Influence of Bi for $n=0.5, B=1, R=0.5,$ $\alpha=\pi/4, Sc=0.22,\ Kr=0,\ R=0.5, Pr=0.71, N=0.5, S=0$

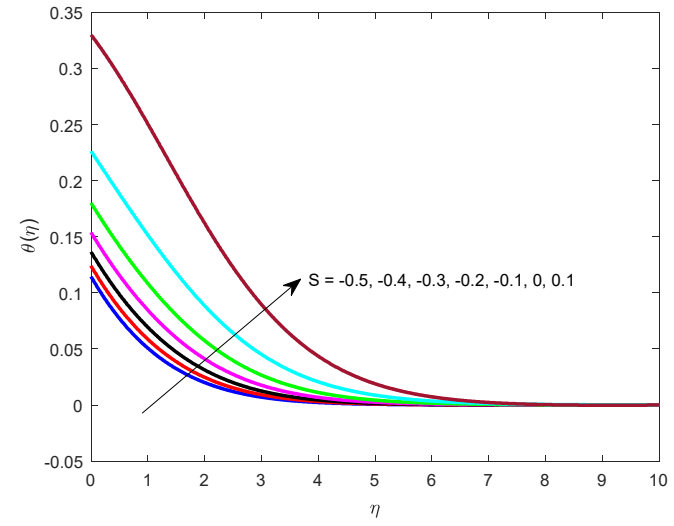

Fig. 12. Behaviour of S for $n=0.5, B=1, R=0.5,$ $\alpha=\pi/4, Sc=0.22,\ Kr=0,\ R=0.5, Pr=0.71, N=0.5, Bi=0.1$

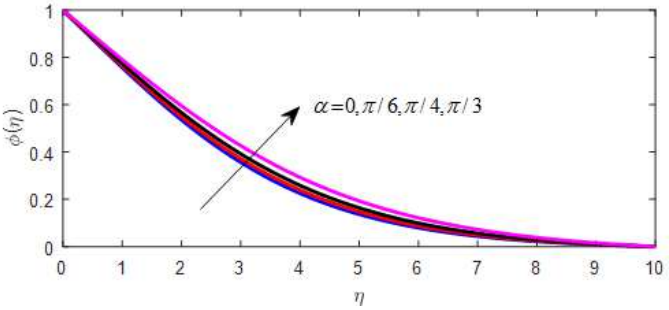

Fig. 13. Variation of α for $n=0.5, B=1, R=0.5,$ $f_w=0.1, Sc=0.22,\ Kr=0,\ Bi=0.1, Pr=0.71, S=0, N=0.5$

3.2. Microrotation profiles

Fig. 5 presents the microrotation profile for various values of material parameter for the presence / absence of other pertinent parameter characterizes the flow phenomena are shown in the figure caption. The trend of microrotation profile is opposite that of the velocity profile near the plate for increasing values of material parameter as presented in Fig. 2. Both the case of Newtonian fluid $(N = 0)$ and non-Newtonian fluid $(N > 0)$ are also presented in the same figure. It is seen that in case of Newtonian fluid the angular velocity is lower than that of non-Newtonian fluid and it is well agrees with the result of Ram Reddy et al. [19]. As the profile increases for $N > 0$, the boundary layer thickness decreases significantly. The interesting observation is that, the profiles of angular velocity leaning towards the negative direction in its domain. Fig. 6 shows the effect of α on the microrotation profiles. Starting from a negative value the angular velocity of the profile increases upto a region $\eta < 1.5$ (approx.) as a result the velocity boundary layer decreases. It is observed that the profile intersects at $\eta = 1.5$ (approx.) and after this layer transition state occurs for which the reverse effect is remarked. The effect of suction/ injection on the microrotation profile is shown in the Fig. 7. In a close comparison with velocity profile it is seen that the effect is reversed. The rise in angular velocity is rapid near the plate within a boundary region of $\eta = 3$ (approx.) as there is an increase in suction but injection retards there at. Further, angular velocity has an opposite character after that region ($\eta > 3$) and then it becomes streamlined to meet the boundary condition.

3.3 Temperature profiles

Fig. 8 shows the effect of α on the temperature profiles for various values of other parameters and the absence of heat source/sink $(S = 0)$ and found to be coincide to Ram Reddy et al. [19] gives a road map for the further investigation in this direction. Also it is remarked that temperature of the micropolar fluid enhances as α increases. From the mathematical point of view it is also evident that as α increases from 0 to $\pi/2$, sin (θ) increases as a result Grashof number increases. Increase in buoyancy force increases the temperature of the fluid. Fig. 9 exhibits the effect of suction/injection on the temperature profiles. It is found that strong suction retards the micropolar fluid temperature hence; the thermal boundary layer subsequently decreases. Further, injection enhances the temperature significantly. Fig. 10 describes the behavior of thermal radiation in the absence of heat source/sink parameter. "*Thermal radiation is an electromagnetic radiation generated by the motion of charged particles in matter*". As any matter having temperature greater than absolute zero emits thermal radiation. "When the temperature of a body is greater than absolute zero, inter-atomic collisions cause the kinetic energy of the atoms or molecules to change". This results an increase in temperature of the polar fluid. Fig. 11 illustrates the effect of Bi on temperature profiles. It is clear to observed that increase in Bi the temperature profile increases significantly. As $Bi \to \infty$, $\theta(0) = 1$ which simulates the isothermal surface. Internal thermal resistance dominates over the boundary layer thermal resistance due to an increase in Biot number therefore, the surface temperature increases. The most important characteristics of the temperature profile is the effect of heat source/sink which is exhibited in Fig. 12. It is to note that the source strength $S\ (S > 0)$ enhances the fluid temperature in a great extent whereas the sink $(S < 0)$ lowers down it significantly. The additional heat source favors to increase the micropolar fluid temperature.

3.4 Concentration profiles

Fig. 13 shows the variation of α due to concentration profile (ϕ) and it is found that ϕ increases as α increases. Significant decrease in ϕ is remarked as an increase in strong suction but impact is reversed for injection (Fig. 14). From Fig. 14 it is noticed that ϕ is asymptotic in nature to meet the inadequate boundary condition. As a result the concentration of the boundary layer also decreases. The behavior of heavier species and chemical reaction parameter on the concentration profiles is shown in Fig. 15. The case of destructive $(Kr > 0)$, constructive $(Kr < 0)$ and no chemical reaction $(Kr = 0)$ are also presented in the same profile. The dotted line represents the lower species concentration i.e. $Sc = 0.22$ and bold represents the higher i.e. $Sc = 0.78$. It is interesting to observe that the fluid concentration decelerates from constructive to destructive significantly whereas low species concentration is favorable to enhance it.

3.5 Tabular Results

Table 1 presents the numerical values of the local skin friction, couple stress coefficient, Nusselt number, Sherwood number for different values of pertinent parameters. In case of $N = 0$ (Newtonian fluid), absence of surface condition parameter, heat source/sink and chemical reaction the present result is satisfied with an earlier published result of Ram Reddy et al. [19]. Also, in case non-Newtonian fluid $(N = 0.5)$ and the absence of these above parameters, all the coefficients of physical quantities of interest decrease in magnitude. Increase in suction all the coefficients increase except Sherwood number whereas injection retards all the coefficients significantly. Radiation parameter enhances all the quantities except the Nusselt number. Constructive chemical reaction parameter decreases the Sherwood number but destructive reaction is to enhance it significantly. Further, sink increases Nusselt number but the source strength decreases it. However heavier species concentration is favoring to increase the rate of mass transfer of micropolar fluid.

4. Concluding remarks

Free convection of micropolar fluid in an inclined permeable surface is investigated in the present analysis. In addition to that the behaviour of heat source/sink along with chemical reaction also enhances the study as well. As a novelty, Lie group transformation is used and the solution of transformed ODEs is obtained numerically. The behaviour of contributing parameters are obtained and presented via graphically and the coefficients for the engineering interest are presented in tabular form. However, from the discussion the following concluding remarks are obtained:

- Validation of the present result in particular case is a benchmark solution for further investigation.
- Angular velocity remains negative in the boundary layer for both assisting and opposing cases.
- Buoyancy assisting and opposing flow are favourable to enhance the fluid temperature.
- The rate of energy transport to the fluid and the values of temperature distribution are raised as an increase in radiation parameter.
- An increase in Soret number, concentration of the fluid increases.
- Constructive reactant coefficient is favourable to enhance the mass transfer rate.

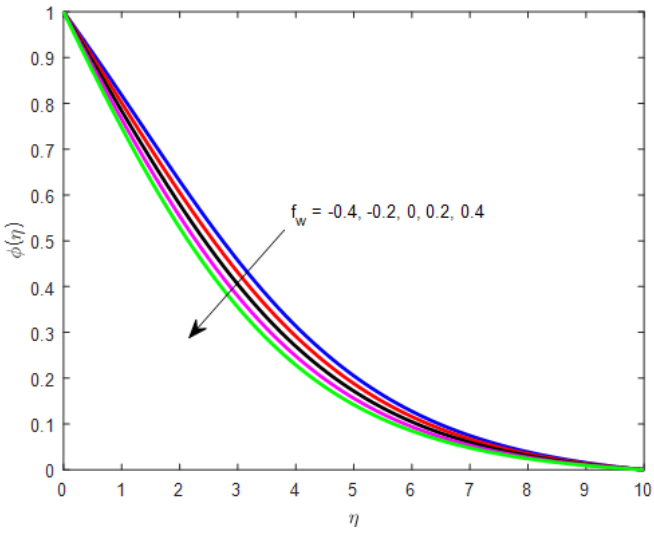

Fig. 14. Influence of f_w for $n = 0.5, B = 1, R = 0.5,$ $\alpha = \pi / 4, Sc = 0.22,\ Kr = 0,\ Bi = 0.1, Pr = 0.71, S = 0, N = 0.5$

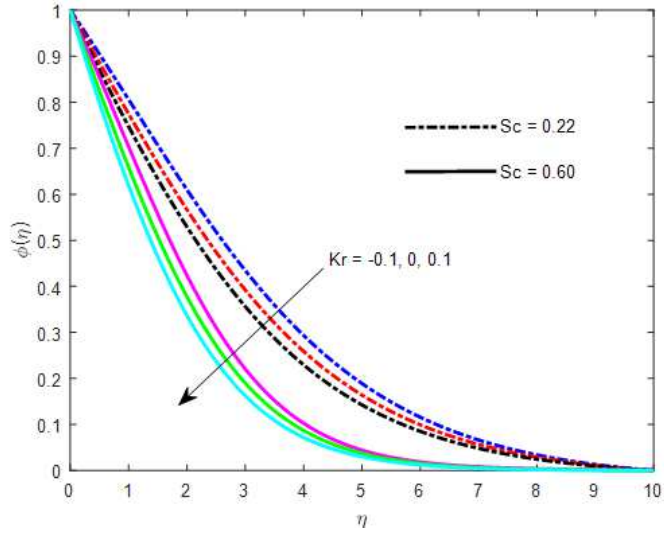

Fig. 15. Influence of Sc and Kr for $n = 0.5, B = 1, R = 0.5, \alpha = \pi / 4,$ $R = 0.5, Pr = 0.71, N = 0.5, Bi = 0.1$

Table 1. Coefficient of physical quantities of interests ($Pr = 0.71, Bi = 0.1, B = 1$ fixed)

N	n	α	f_w	R	Sc	Kr	S	$f'(0)$	$h'(0)$	$-\theta'(0)$	$-\varphi'(0)$
0	0	$\pi/2$	0.1	0.5	0.22	0	0	2.6573667	8.4615193	0.0556598	0.111403
0		$\pi/4$						0.8893763	-0.444688	0.0782222	0.2370888
0.5								0.6779733	-0.338987	0.0773751	0.2290111
	0.5							0.6779733	-0.338987	0.0773751	0.2290111
	1.5							1.1096598	-1.66449	0.0790626	0.2483065
	0.5		0					0.6704779	-0.335239	0.0759218	0.2174584
			-0.1					0.6629606	-0.33148	0.0743411	0.2062957
			0.1	0.3				0.6711521	-0.335576	0.0785741	0.2281409
				0.1				0.6637289	-0.331864	0.0799077	0.2272447
				0.5	0.6			0.6056885	-0.302844	0.075762	0.3560022
					0.78			0.5853579	-0.292679	0.0752676	0.4007132
					0.22	-0.1		0.6944734	-0.347237	0.077656	0.1871738
						0.1		0.6634934	-0.331747	0.0771155	0.2668805
							-0.1	0.6552557	-0.327627	0.0819978	0.2265443
							0.1	0.7281890	-0.364095	0.0670013	0.2345577

Author Contributions

A.K. Dash planned the scheme, initiated the work and suggested the model; S.R. Mishra conducted the methodology and examined the theoretical validation of the manuscript and all authors discussed the results, reviewed and approved the final version of the manuscript.

Acknowledgments

The authors are very much thankful to the learned reviewers for their qualitative suggestions to improve the quality of our manuscript.

Conflict of Interest

The authors declared no potential conflicts of interest with respect to the research, authorship and publication of this article.

Funding

The authors received no financial support for the research, authorship and publication of this article.

Data Availability Statements

The datasets generated and/or analyzed during the current study are available from the corresponding author on reasonable request.

References

[1] Eringen, A. C., The theory of Micropolar fluids, *Journal of Mathematics and Mechanics*, 16, 1966, 1-18
[2] Eringen, A. C., Theory of thermomicropolar fluids, *Journal of Mathematical Analysis and Applications*, 38, 1972, 480-496.
[3] Ahmadi, G., Self similar solution of incompressible micropolar boundary layer flow over a semi-infinite plate, *International Journal of Engineering*

Science, 14, 1976, 639-646.
[4] Carragher, P., Crane, L. J., Heat transfer on a continuous stretching sheet, *Zeitschrift für Angewandte Mathematik und Mechanik,* 62, 1982, 564–565.
[5] Chim, K. E., Nazar, R., Arifin, N.M., Pop, I., Effect of variable viscosity on mixed convection boundary layer flow over a vertical surface embedded in a porous medium, *International Communications in Heat and Mass Transfer,* 34(4), 2007, 464–473.
[6] Chamkha J. A., MHD-free convection from a vertical plate embedded in a thermally stratified porous medium with Hall effects, *Appl. Math. Modelling,* 21, 1997, 603-609.
[7] Beg, O. A., Bhargava, R., Rawat, S., Takhar, H. S., Beg T. A., Study of Steady Buoyancy-Driven Dissipative Micropolar Free Convection Heat and Mass Transfer in a Darcian Porous Regime with Chemical Reaction, *Nonlinear Analysis: Modelling and Control,* 12, 2007, 157–180.
[8] Rawat, S., Bhargava, R., Finite element study of natural convection heat and mass transfer in a micropolar fluid-saturated porous regime with soret/dufour effects, *Int. J. Appl. Math Mech.*, 5(2), 2009, 58-71.
[9] Hayat, T., Mustafa, M., Pop, I., Heat and mass transfer for Soret and Dufour's effect on mixed convection boundary layer flow over a stretching vertical surface in a porous medium filled with a visco-elastic fluid, *Communications in Nonlinear Science and Numerical Simulation,* 15(5), 2010, 1183–1196.
[10] Mukhopadhyay, S., Effect of thermal radiation on unsteady mixed convection flow and heat transfer over a porous stretching surface in porous medium, *International Journal of Heat and Mass Transfer,* 52(13), 2009, 3261–3265.
[11] Rahman, M. M., Sattar, M. A., MHD convective flow of a micro polar fluid past a continuously moving vertical porous plate in the presence of heat generation/absorption, *J. Heat Transfer,* 17, 2006, 85-90.
[12] Reddy, C. V. R., Murthy, C. H. V. R., Reddy, N. B., Unsteady MHD free convective mass transfer flow past an infinite vertical porous plate with variable suction and Soret effect, *Int. J. Appl. Math Mech.*, 7(21), 2011, 70-84.
[13] Rawat, S., Bhargava, R., Kapoor, S., Beg, O. A., Heat and Mass Transfer of a Chemically Reacting Micropolar Fluid Over a Linear Streaching Sheet in Darcy Forchheimer Porous Medium., *International Journal of Computer Applications*, 44 (6), 2012, 40-51.
[14] Tripathy, R. S., Dash, G. C., Mishra, S. R., Baag, S., Chemical reaction effect on MHD free convective surface over a moving vertical plane through porous medium, *Alexandria Engineering Journal,* 54 (3), 2015, 673-679.
[15] Tripathy, R. S., Mishra, S. R., Dash, G. C., Hoque, M. M., Numerical analysis of hydromagnetic micropolar fluid along a stretching sheet with non-uniform heat source and chemical reaction, *Engineering Science and Technology, An International Journal,* 19(3), 2016, 1573-1581.
[16] Mishra, S. R., Baag, S., Mohapatra, D. K., Chemical reaction and Soret effects on hydromagnetic micropolar fluid along a stretching sheet, *Engineering Science and Technology, An International Journal,* 19(4), 2016, 1919-1928.
[17] Baag, S., Mishra, S. R., Dash, G. C., Acharya, M. R., Numerical investigation on MHD micropolar fluid flow toward a stagnation point on a vertical surface with heat source and chemical reaction, *Journal of King Saud Engineering Sciences*, 29, 2017, 75-83.
[18] Mishra, S. R., Hoque, M. M., Mohanty, B., Heat transfer effect on MHD flow of a micropolar fluid through porous medium with uniform heat source and radiation, *Nonlinear Engineering – Modeling and Application,* 8(1), 2019, 65-73.
[19] Ram Reddy, Ch., Murthy, P. V. S. N., Chamkha, A. J., Rashad, A. M., Soret effect on mixed convection flow in a nanofluid under convective boundary condition, *International Journal of Heat and Mass Transfer*, 64, 2013, 384-392.

ORCID iD

A.K. Dash https://orcid.org/0000-0002-4391-5548
S.R. Mishra https://orcid.org/0000-0002-3018-394X

How to cite this article: Dash A.K., Mishra S.R. Free Convection of Micropolar Fluid over an Infinite Inclined Moving Porous Plate, *J. Appl. Comput. Mech.*, 8(4), 2022, 1154–1162. https://doi.org/10.22055/JACM.2021.16703